Journal of Electrocardiology 63 (2020) 159–163

Contents lists available at ScienceDirect

Journal of Electrocardiology

journal homepage: www.jecgonline.com

Fully automated QRS area measurement for predicting response to cardiac resynchronization therapy

Filip Plesinger [a], Antonius M.W. van Stipdonk [b], Radovan Smisek [a], Josef Halamek [a], Pavel Jurak [a], Alexander H. Maass [c], Mathias Meine [d], Kevin Vernooy [b], Frits W. Prinzen [e,*]

[a] Institute of Scientific Instruments of the Czech Academy of Sciences, Brno, Czech Republic
[b] Department of Cardiology, Maastricht University Medical Center, Maastricht, the Netherlands
[c] Department of Cardiology, University of Groningen, University Medical Centre Groningen, Groningen, the Netherlands
[d] Department of Cardiology, University Medical Centre Utrecht, Utrecht, the Netherlands
[e] Department of Physiology, Cardiovascular Research Institute Maastricht (CARIM), Maastricht, the Netherlands

ARTICLE INFO

Article history:
Received 2 May 2019
revised 18 June 2019
accepted 6 July 2019

Keywords:
Heart failure
Cardiac resynchronization therapy
Vectorcardiography
QRS area
Software
Signal averaging

ABSTRACT

Background: Cardiac resynchronization therapy (CRT) is an established treatment in patients with heart failure and conduction abnormalities. However, a significant number of patients do not respond to CRT. Currently employed criteria for selection of patients for this therapy (QRS duration and morphology) have several shortcomings. QRS area was recently shown to provide superior association with CRT response. However, its assessment was not fully automated and required the presence of an expert.
Objective: Our objective was to develop a fully automated method for the assessment of vector-cardiographic (VCG) QRS area from electrocardiographic (ECG) signals.
Methods: Pre-implantation ECG recordings (N = 864, 695 left-bundle-branch block, 589 men) in PDF files were converted to allow signal processing. QRS complexes were found and clustered into morphological groups. Signals were converted from 12-lead ECG to 3-lead VCG and an average QRS complex was built. QRS area was computed from individual areas in the X, Y and Z leads. Practical usability was evaluated using Kaplan-Meier plots and 5-year follow-up data.
Results: The automatically calculated QRS area values were 123 ± 48 μV.s (mean values and SD), while the manually determined QRS area values were 116 ± 51 ms; the correlation coefficient between the two was r = 0.97. The automated and manual methods showed the same ability to stratify the population (hazard ratios 2.09 vs 2.03, respectively).
Conclusion: The presented approach allows the fully automatic and objective assessment of QRS area values.
Significance: Until this study, assessing QRS area values required an expert, which means both additional costs and a risk of subjectivity. The presented approach eliminates these disadvantages and is publicly available as part of free signal-processing software.

Introduction

Cardiac resynchronization therapy (CRT) is an effective way of treating heart failure patients. Several approaches have been proposed in the past to predict response to CRT, leading to the current guidelines for selection of patients for this therapy [1,2] using QRS morphology and QRS duration. Nevertheless, even using these guidelines approximately 30% of patients do not show a recognizable response to CRT [3–5]. As reviewed recently [6] there are several potential reasons for this disappointing number. A) QRS duration may be prolonged due to various abnormalities, which not all are amenable to CRT, B) measurement of QRS duration is less accurate than assumed, C) there are multiple definitions of LBBB and it requires subjective judgement. The latter leads to considerable variability between observers and even within observers [7]. D) Moreover, LBBB has been defined to describe a certain conduction abnormality, but not as a marker of CRT response. In search for a better marker of dyssynchrony we recently showed that QRS area was associated with echocardiographic response to CRT [8]. Moreover, QRS area was associated even better with the clinical outcome of CRT patients than even the combination of QRS duration and the LBBB morphology of the QRS complex [9–11].

However, in these studies QRS area measurement has been performed semi-automatically which still makes it partly subjective

* Corresponding author at: Department of Physiology, Cardiovascular Research Institute Maastricht, Maastricht University, P.O. Box 616, 6200 MD Maastricht, the Netherlands.
E-mail address: frits.prinzen@maastrichtuniversity.nl (F.W. Prinzen).

https://doi.org/10.1016/j.jelectrocard.2019.07.003

and, first and foremost, time-consuming. Here, we present a fully automated approach to the measurement of QRS area and related variables and an evaluation of the results obtained in a large database containing follow-up data.

Materials and methods

Retrospective ECG data from 865 patients (589 men) from the multicentric MUG database [9] were used. This retrospective cohort consists of patients with heart failure (NYHA class II-IV, LV ejection fraction <35%) and a wide QRS complex (QRS duration >120 ms), qualifying them for de novo CRT implantation, for whom long-term follow-up data was available. Their baseline ECGs were stored as PDF files on ECG recording equipment (MAC 5500 ECG Machine by GE Healthcare, Waukesha, WI, USA), containing at least one common running lead, at a speed of 25 mm/s. ECGs were acquired prior to CRT (duration 10 s in the supine position, 12-lead, sampling frequency 250 Hz or 500 Hz). The mean age was 66.8 ± 11.0 years. A total of 695 patients were recognized as having left-bundle-branch block (LBBB) by the criteria of the European Society of Cardiology (ESC). The endpoint of clinical outcome to CRT was a combination of death, cardiac transplantation or left ventricular assist device (LVAD) implantation within 5 years of CRT [9].

Method

Digital 12-lead ECG signals were extracted from the PDF files (Fig. 1, top). This was performed in several batches – from PDF to SVG (Scalable Vector Graphics file format) using Adobe Illustrator and then from SVG into CSV file format using a custom-made convertor. Finally, signals in CSV files were processed fully automatically in SignalPlant [12] software (Fig. 1, B–K).

Using the digital 12-lead ECG, derived as described above, but basically using any digital 12-lead ECG, QRS complexes can be detected [13] using amplitude envelograms (Fig. 1B). In our case, within the ~10-second recording, signals were filtered (FIR filter, band-pass 8–30 Hz, Fig. 1C) and QRS complexes were clustered into groups by morphology [14] (Fig. 1D). If the source PDF file used the common clinical 3 × 4 leads setup (Fig. 1E), signals were reconstructed using one or more running leads (Fig. 1F). Next, the data was transformed (Fig. 1G) to Frank orthogonal leads using Kors' approach, thereby creating vector-cardiogram (VCG) signals [15].

Next, the X, Y and Z signals were filtered (FIR filter, low-pass at 30 Hz, Fig. 1H). The averaged QRS beat was computed (Fig. 1I) using QRS annotation marks as a trigger. In order to exclude extrasystoles, only QRS complexes belonging to the most common morphological group were used to compute the average QRS complex; beats were averaged in the range of <—0.2 to 0.2 s> from the QRS annotation marks (Fig. 2A).

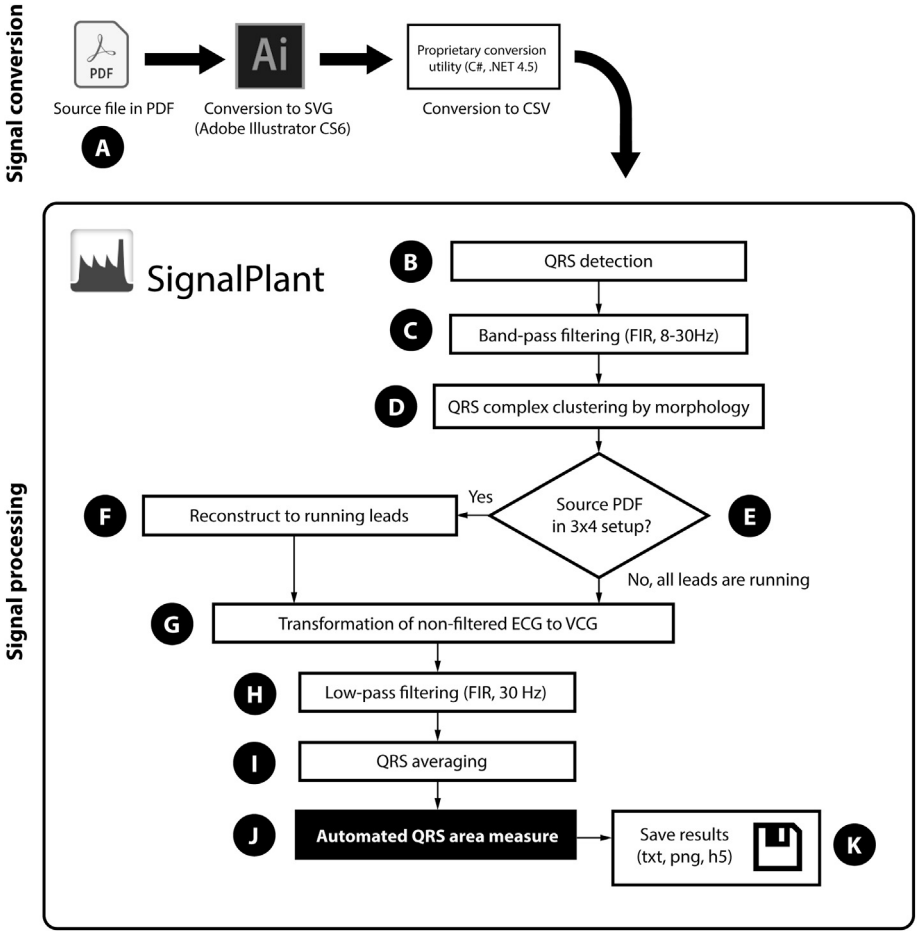

Fig. 1. Data processing toolchain. Source ECG signals were converted from PDF file format (A) to Scalable-Vector-Graphics (SVG) format and, finally, using a custom-made convertor, into CSV files. CSV files were loaded into SignalPlant [11] processing software where all signal processing was performed in a batch. QRS complexes were detected (B), signals were filtered (C) and QRS complexes were clustered by morphology into morphological groups (D). Files saved in the common cardiologic setup of 3 × 4 panels had to been converted into running-leads setup (E, F). ECG signals were converted into vector-cardiographic signals (G), filtered (H), and the averaged beat from the most common morphological group was obtained (I). Finally, the automated QRS area measurement was executed (J, see Fig. 2 for more details) and the results were saved for further processing (K).

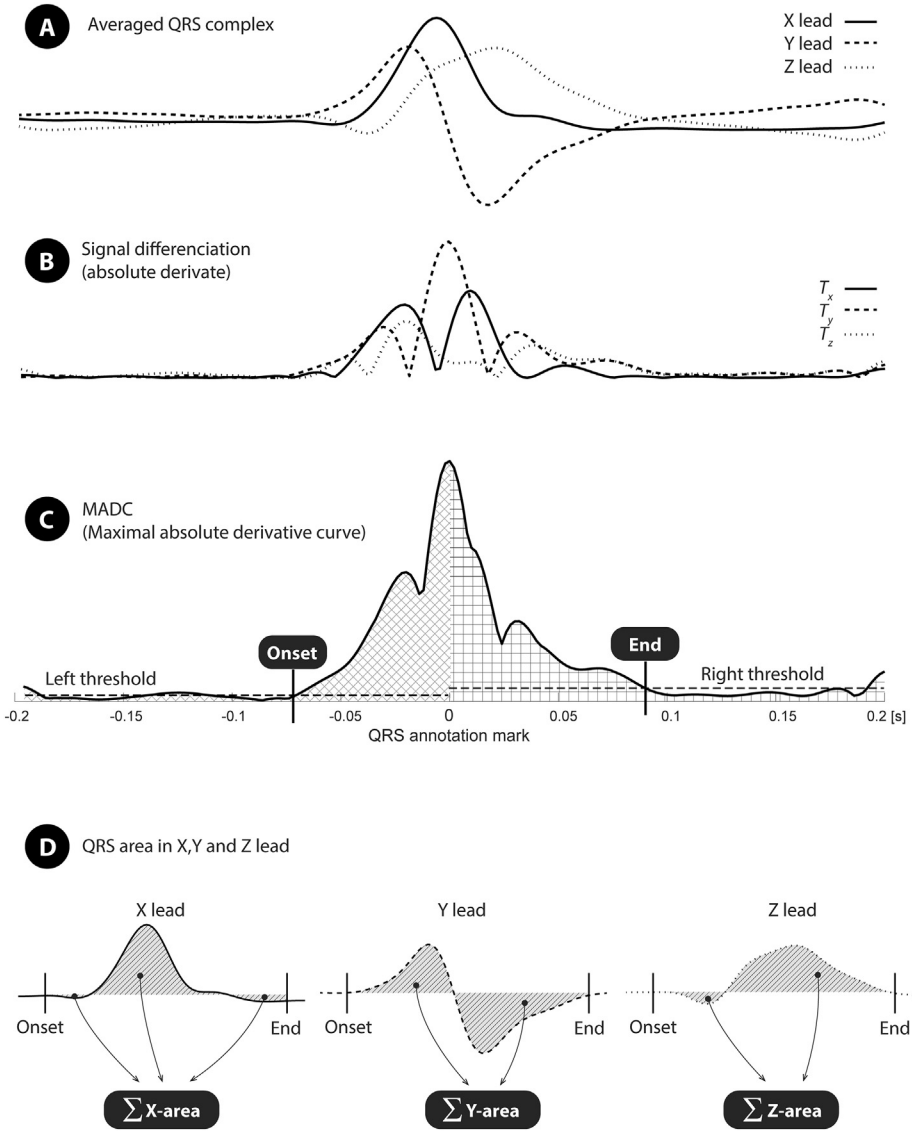

Fig. 2. Automated QRS area measurement. The averaged QRS complex using Frank orthogonal leads (A) is transformed (B, Eq. (1)) and single curve (C, MADC) is computed from TX, TY and TZ transformed signals (Eq. (2)). The left and right thresholds (C, dashed horizontal lines) are defined as the median value of the left (from −0.2 to 0 s) and right (from 0 to 0.2 s) half of MADC, respectively. QRS onset and end are found where the median of the floating window (0.025 s) drops below these thresholds. Finally, QRS areas in X-Y-Z leads are found (D, hatched areas) and are used to compute the QRS area (Eq. (3)).

The automated measurement of QRS area (Fig. 1J, detail in Fig. 2) requires the detection of QRS onset and end. We designed an approach for defining QRS onset and end which, unlike the conventional approach, uses exhaustive information related to small voltage amplitudes usually invisible on standard millimeter paper. As a consequence, QRS onset and end are tracked more subtly. We seek locations close to the QRS annotation mark where the signal starts/stops to change (for this purpose the 1st derivative of the VCG signal is considered); we also combine information from multiple leads. The entire procedure is illustrated in Fig. 2 and explained more specifically below: VCG signals from the averaged QRS complex (Fig. 2A) were differentiated and each sample was transformed to its absolute value:

$$T_x = |diff\ (x)|; T_y = |diff\ (y)|; T_z = |diff\ (z)| \quad (1)$$

where x, y and z are signals from orthogonal leads from the averaged QRS complex; resultant transformed signals T_x, T_y and T_z are shown in Fig. 2B. Next, the maximal values of these transformed leads formed the Maximal Absolute Derivative curve (*MADC*, Fig. 2C). Each *i*-th sample of *MADC* was therefore computed as:

$$MADC_i = max\ (T_{x,i}; T_{y,i}; T_{z,i}) \quad (2)$$

The median value of the left half of the *MADC* (Fig. 2C, from −0.2 to 0 s) was used as a threshold for QRS onset, while the median value of the right half of the *MADC* (Fig. 2C, from 0 to 0.2 s) served as a threshold for the end of the QRS complex (Fig. 2C – dashed horizontals). Finally, QRS onset and end were found where the median *MADC* value in a short floating window (0.025 s) dropped below the corresponding threshold (Fig. 2C – verticals).

When QRS onset and end were found, the QRS area value was computed from the summed areas above and below the baseline (defined by the nominal value at onset) in the X, Y and Z leads (Fig. 2D) as:

$$QRS_{area} = \sqrt{X_{area}^2 + Y_{area}^2 + Z_{area}^2} \quad (3)$$

Results of this automated analysis were compared with those acquired by the manual method employed in Maastricht [16]. In brief,

Table 1
The study results showed significant stratification power for both the presented and the reference approach; these results are shown as hazard ratios, their significance and Chi-squares using 5-year follow-up data. CI – confidence interval. SD – standard deviation. QRS area values are presented in [μV.s].

	Automated	Manual/expert	Difference
Number of cases	864	864	864
QRS area Mean ± SD	123 ± 48	116 ± 51	5.6 ± 12.7
QRS area median	116	111	–
(25th, 75th percentile)	(87, 152)	(78, 150)	
Hazard ratio (95% CI)	2.09 (1.52–2.79)	2.03 (1.49–2.72)	–
Significance (Log-rank)	$p < 0.0001$	$p < 0.0001$	
Chi-square χ^2	22.02	20.56	–
Pearson correlation	$r = 0.97$		–

for each individual ECG the vector graphics of the PDF file were obtained by converting the files to an .svg file using Inkscape version 2 (Boston, MA, USA). The digital ECG signals were semi-automatically analyzed using a custom-made computer program written in MATLAB R2010b (MathWorks, Natick, MA). After band-pass filtering between 0.5 and 40 Hz and baseline wander removal, the beginning and end of the QRS complex were detected using the curve length transformation (cLT). The beginning of the QRS complex corresponded to the last found minimum value and the end of the QRS complex was the first point with maximal cLT value. Subsequently, custom MATLAB software was used to convert the 12-lead ECG into the three orthogonal VCG leads (X-, Y-, and Z-) using the Kors conversion matrix. QRS area was calculated as the sum of the area under the QRS complex in the calculated vectorcardiographic X, Y and Z lead [QRS area $= (QRS^2_{area,x} + QRS^2_{area,y} + QRS^2_{area,z})^{1/2}$] [16].

Statistical analysis

Automatically obtained values of QRS area were statistically processed in GraphPad Prism ver. 6. Association between automated and manual [16] QRS area values was tested using Pearson correlation. The ability to stratify the population into responding and non-responding groups was shown using Kaplan-Meier [17] plots and quantified as the cumulative hazard ratio and Chi-square (χ^2). The significance of stratification was tested using a log-rank test.

Results

The method has been implemented as an update to the averaging plugin for the free SignalPlant [12] processing software (plugin name: "Compare averaged shapes"). The plugin can be controlled in batch operation, and this was used for the data processing in this paper. It can also be used with GUI, allowing manual inspection.

The results for all 865 recordings are shown in Table 1. The Pearson correlation of the QRS area between the fully automatically and manually acquired values was $r = 0.97$ ($p < 0.0001$). The automated analysis provided larger values for QRS area (123 ± 48 vs 116 ± 51 μV.s). The

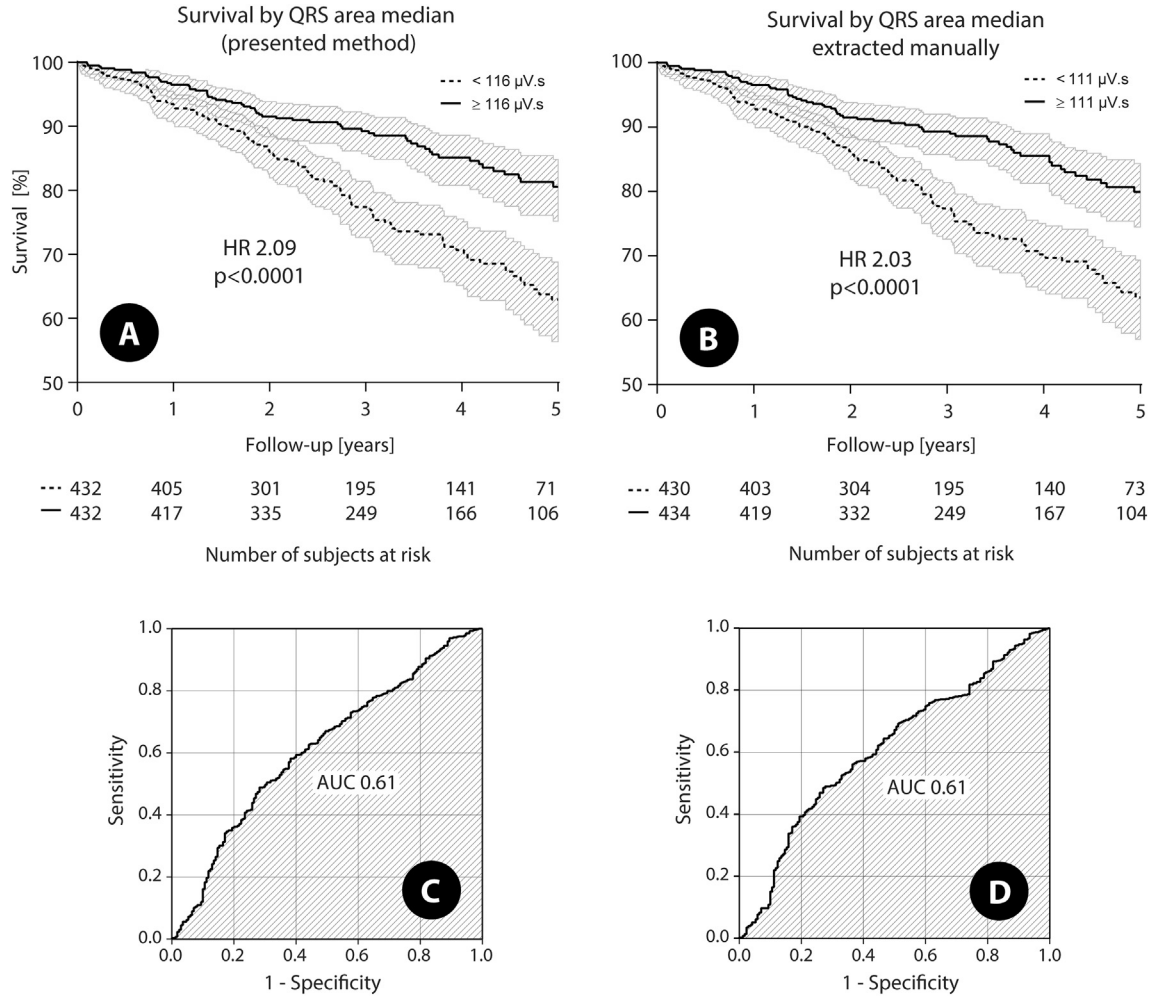

Fig. 3. Kaplan-Meier plots for QRS area (A and B) and ROC curves (C and D) assessed by the automated (A, C) and manual (B,D) approach. The population was stratified using median values of corresponding variables (see Table 1). 5-year survival based on QRS area measurements showed nearly the same stratification power for both automated and manual measurement, though slightly in favor of the presented approach. Hatched areas reflect 95% confidence intervals.

delay measured between QRS onset and end was 175 ± 17 ms; its correlation with expert QRS duration was 0.62 which reflects the fact that our approach implements criteria technically invisible to experts.

In terms of clinical outcome, we examined the relationship between both the manually and automatically determined QRS area and patient survival during CRT using Kaplan-Meier plots [17] (Fig. 3). Data was stratified using the median values over the whole population (116 μV.s and 111 μV.s for automated and manual QRS area values, respectively). The results for the manual analysis were congruent with a prior analysis on a larger number of patients in the same database [9]. The automated analysis showed a quite similar result as that for the manual analysis: survival curves showed Chi-square (χ^2) values of 22.02 and 20.56 for the automated and manual approach, respectively and hazard ratios (HR) of 2.09 (95% CI 1.52–2.79) and 2.03 (95% CI 1.49–2.72) for the automated and manual approach, respectively.

Discussion

The aim of this paper was to present a method for fully automated measurement of QRS area. Our results show that automated and manual QRS area values are strongly correlated and provide similar prediction of outcome after CRT using baseline VCG.

Implications

Based on the results it can be stated that the presented algorithm is reliable. This finding is important because the method presented here can be easily implemented in offline analysis and, potentially, also in medical devices which will allow easier, faster and user-independent measurement of QRS area. This parameter is increasingly regarded as a valuable addition to the ECG measurements that are used to select patients for CRT [9,11], though the specific analysis required until now may discourage investigators and clinicians from using it. Once QRS area can be used easily, it may also become feasible to include it in the guidelines for the selection of CRT patients.

Limitations

Several limitations should be mentioned. First of all, 4 recordings could not be automatically processed (the criteria for stating QRS onset and/or end were not met) and, therefore, were excluded from the analysis. In the present study, we only analyzed pre-implantation recordings without pacemaker activity. However, looking into other conditions, we have found that the pacing artefact can confuse the detection of onset of the QRS complex. Therefore, an algorithm to remove this artefact should be applied when paced beats are analyzed. We have also found that delay between QRS onset and end using the automated approach is different from conventionally determined QRS duration. The implications of this should be further investigated.

Conclusion

We have presented an algorithm for fully automated assessment of QRS area. It was shown that QRS area values produced with the presented method are as useful as manually assessed values, as demonstrated by the survival stratification of CRT patients. Therefore, the presented QRS area analysis may be fully automated which facilitates both analysis of large cohorts of patients and continuous remote monitoring. The presented algorithm is publicly available as a plugin for SignalPlant processing software (www.signalplant.org).

Declaration of Competing Interest

A.H.M reports lecture fees from Medtronic and Microport CRM. K.V. reports consultancy for Medtronic; research grants from Medtronic; speaker fees from Abbott. F.W.P. reports research grants from Medtronic, Abbott, Biotronik, Microport CRM, Biosense Webster and EBR Systems.

Acknowledgements

This study was supported by the Czech Academy of Sciences, grant MSM100651602; by the Czech Science Foundation, project GA17-13830S; and by the Ministry of Education, Youth and Sports of the Czech Republic, project LO1212.

References

[1] Brignole M, Aurichio A, Baron-Esquivias G, Bordachar P, Boriani G, Breithardt O, et al. 2013 ESC Guidelines on cardiac pacing and cardiac resynchronization therapy. Eur Heart J 2013;34:2281–329. https://doi.org/10.1093/eurheartj/eht150.
[2] Tracy CM, Epstein AE, Darbar D, DiMarco JP, Dunbar SB, Estes NAM, et al. 2012 ACCF/AHA/HRS focused update incorporated into the ACCF/AHA/HRS 2008 guidelines for device-based therapy of cardiac rhythm abnormalities. J Am Coll Cardiol 2013;61:e6–75. https://doi.org/10.1016/j.jacc.2012.11.007.
[3] Varma N, Manne M, Nguyen D, He J, Niebauer M, Tchou P. Probability and magnitude of response to cardiac resynchronization therapy according to QRS duration and gender in nonischemic cardiomyopathy and LBBB. Heart Rhythm 2014;11:1139–47. https://doi.org/10.1016/j.hrthm.2014.04.001.
[4] Dupont M, Rickard J, Baranowski B, Varma N, Dresing T, Gabi A, et al. Differential response to cardiac resynchronization therapy and clinical outcomes according to QRS morphology and QRS duration. J Am Coll Cardiol 2012;60:592–8. https://doi.org/10.1016/j.jacc.2012.03.059.
[5] Vidula H, Kutyifa V, McNitt S, Goldenberg I, Solomon SD, Moss AJ, et al. Long-term survival of patients with left bundle branch block who are hypo-responders to cardiac resynchronization therapy. Am J Cardiol 2017. https://doi.org/10.1016/j.amjcard.2017.06.001.
[6] Engels EB, Mafi-Rad M, van Stipdonk AMW, Vernooy K, Prinzen FW. Why QRS duration should be replaced by better measures of electrical activation to improve patient selection for cardiac resynchronization therapy. J Cardiovasc Transl Res 2016;9:257–65. https://doi.org/10.1007/s12265-016-9693-1.
[7] van Stipdonk AMW, Vanbelle S, ter Horst IAH, Luermans JG, Meine M, Maass AH, et al. Large variability in clinical judgement and definitions of left bundle branch block to identify candidates for cardiac resynchronisation therapy. Int J Cardiol 2019. https://doi.org/10.1016/j.ijcard.2019.01.051.
[8] Maass AH, Vernooy K, Wijers SC, van't Sant J, Cramer MJ, Meine M, et al. Refining success of cardiac resynchronization therapy using a simple score predicting the amount of reverse ventricular remodelling: results from the markers and response to CRT (MARC) study. EP Europace 2018;20:e1–10. https://doi.org/10.1093/europace/euw445.
[9] van Stipdonk AMW, Ter Horst I, Kloosterman M, Engels EB, Rienstra M, Crijns HJGM, et al. QRS area is a strong determinant of outcome in cardiac resynchronization therapy. Circ Arrhythm Electrophysiol 2018;11:e006497. https://doi.org/10.1161/CIRCEP.118.006497.
[10] Van Deursen CJM, Vernooy K, Dudink E, Bergfeldt L, Crijns HJGM, Prinzen FW, et al. Vectorcardiographic QRS area as a novel predictor of response to cardiac resynchronization therapy. J Electrocardiol 2015. https://doi.org/10.1016/j.jelectrocard.2014.10.003.
[11] Emerek K, Friedman DJ, Sørensen PL, Hansen SM, Larsen JM, Risum N, et al. Vectorcardiographic QRS area is associated with long-term outcome following cardiac resynchronization therapy. Heart Rhythm 2018;16:213–9. https://doi.org/10.1016/j.hrthm.2018.08.028.
[12] Plesinger F, Jurco J, Halamek J, Jurak P. Signal plant: an open signal processing software platform. Physiol Meas 2016;37:N38–48.
[13] Plesinger F, Jurco J, Jurak P, Halamek J. Robust multichannel QRS detection. Comput Cardiol 2010;41:2014.
[14] Plesinger F, Jurco J, Halamek J, Leinveber P, Reichlova T, Jurak P. Multichannel QRS morphology clustering data preprocessing for ultra-high-frequency ECG analysis. CARDIOTECHNIX 2015 - Proc. 3rd Int. Congr. Cardiovasc. Technol; 2015.
[15] Kors JA, Van Herpen G, Sittig AC, Van Bemmel JH. Reconstruction of the frank vectorcardiogram from standard electrocardiographic leads: diagnostic comparison of different methods. Eur Heart J 1990. https://doi.org/10.1093/oxfordjournals.eurheartj.a059647.
[16] Engels EB, Végh EM, Van Deursen CJM, Vernooy K, Singh JP, Prinzen FW. T-wave area predicts response to cardiac resynchronization therapy in patients with left bundle branch block. J Cardiovasc Electrophysiol 2015;26:176–83. https://doi.org/10.1111/jce.12549.
[17] Kaplan, Edward L, Meier P. Nonparametric estimation from incomplete observations. J Am Stat Assoc 1958;53:457–81. https://doi.org/10.2307/2281868.